

Cite this: *Dalton Trans.*, 2012, **41**, 10930

www.rsc.org/dalton

## Synthetic and catalytic intermediates in a magnesium promoted Tishchenko reaction†

Benjamin M. Day,<sup>a</sup> William Knowelden<sup>a</sup> and Martyn P. Coles<sup>\*b</sup>

Received 2nd July 2012, Accepted 26th July 2012

DOI: 10.1039/c2dt31442h

Magnesium-aryloxide and -amide compounds supported by amidinate ligands are accessible in two-steps from a suitable Grignard reagent. Both species are active for the dimerization of benzaldehyde. The slower initiation by the aryloxide was exploited in the isolation of a bis-mesitylaldehyde adduct.

The development of compounds capable of promoting the dimerization of aldehydes to esters (the Tishchenko reaction<sup>1</sup>) remains an attractive goal for organic and inorganic chemists.<sup>2</sup> Main group metal compounds have been particularly promising as (pre)catalysts capable of promoting this transformation. For example, Hill and co-workers investigated the activity of heavier group 2 (Ca, Sr, Ba) metal amides,<sup>3</sup> and a homogeneous magnesium thiolate system has recently been studied in detail.<sup>4</sup> Our initial efforts in this area involved the application of magnesium compounds supported by the bicyclic guanidinate ligands, [hpp]<sup>−</sup> and [tbo]<sup>−</sup> (Fig. 1).<sup>5</sup> We showed that the bimetallic complexes **A** and **B** are active pre-catalysts in the Tishchenko reaction, with good activity for the non-enolizable substrates benzaldehyde and pivaldehyde.

The target pre-catalysts in this study combine an ancillary amidinate ligand with a potentially reactive Mg–OR or Mg–NR<sub>2</sub> functionality. Ether solvents were used during the synthesis to provide a source of labile ligands capable of occupying the remaining metal coordination sites, restricting aggregation and promoting the isolation of mononuclear species.

A convenient, atom-efficient synthesis of amidinates is the insertion of a carbodiimide into a metal–carbon bond. This has been demonstrated previously with *p*-block elements,<sup>7</sup> and is particularly attractive for magnesium given the availability of many organometallic precursors in the form of Grignard reagents.<sup>8</sup> Care must be taken, however, as Schlenk equilibria

and ligand redistribution reactions frequently generate the solvated bis-amidinate complex as a stable product.<sup>8,9</sup>

The aryloxide Mg(mesC{NCy}<sub>2</sub>)(OAr)(THF) [**3**, Ar = 2,6-*t*-Bu<sub>2</sub>C<sub>6</sub>H<sub>3</sub>] was synthesized by the sequential addition of *N,N'*-dicyclohexylcarbodiimide and LiOAr to the Grignard reagent Mg(mes)Br (Scheme 1). The order of addition does not affect the formulation of the final product, although a better overall

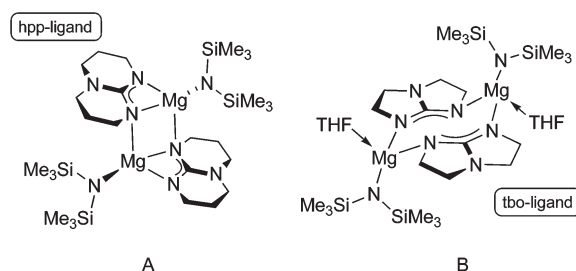
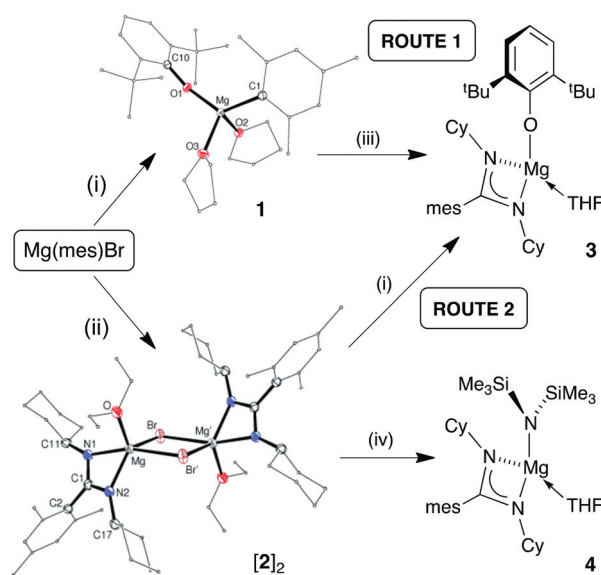


**Fig. 1** Isolated magnesium guanidinate complexes active as pre-catalysts in the Tishchenko reaction. hppH = 1,3,4,6,7,8-hexahydro-2*H*-pyrimido[1,2-*a*]pyrimidine; Htbo = 1,4,6-triaza-bicyclo[3.3.0]oct-4-ene.



**Scheme 1** Synthesis of **1–4** showing the molecular structures of **1** and [**2**]<sub>2</sub>. (i) LiOAr, THF; (ii) CyN=C=NCy, Et<sub>2</sub>O; (iii) CyN=C=NCy, THF; (iv) LiN{SiMe<sub>3</sub>}<sub>2</sub>, THF.

<sup>a</sup>Department of Chemistry, University of Sussex, Falmer, Brighton BN1 9QJ, UK

<sup>b</sup>School of Chemical and Physical Sciences, Victoria University of Wellington, PO Box 600, Wellington, New Zealand.

E-mail: martyn.coles@vuw.ac.nz; Fax: +64 (0) 4 463 5237;

Tel: +64 (0) 4 463 6357

†Electronic supplementary information (ESI) available: Experimental procedures and characterization data for all new compounds, ORTEP representations of **1**, [**2**]<sub>2</sub> and **4**, details of catalytic reactions. CCDC 888956–888960 (for **1–5**). For ESI and crystallographic data in CIF or other electronic format see DOI: 10.1039/c2dt31442h

yield of **1** is achieved by route 2. The products of the first step of the reaction have been isolated in each case and verified as  $\text{Mg}(\text{mes})(\text{OAr})(\text{THF})_2$  (**1**) and  $\text{Mg}(\text{mesC}\{\text{NCy}\}_2)\text{Br}(\text{THF})$  (**2**).

The  $^1\text{H}$  and  $^{13}\text{C}$  NMR spectra of isolated crystals of **1** indicate the formation of a mixture of compounds in solution (ESI† lists data for the dominant species).‡ The related aryloxy bridged dimer  $[\text{Mg}(\mu\text{-OAr})(n\text{-Bu})_2]$  is known to form small amounts of  $\text{Mg}(\text{OAr})_2(\text{THF})_2$  in THF, which in turn can rearrange to form  $[\text{Mg}(\mu\text{-OAr})(\text{OAr})_2]$  and  $[\text{Mg}(\text{OAr})][\text{Mg}(\text{OAr})_3]$ , depending on solvent and conditions.<sup>10</sup> It is probable that **1** is undergoing similar exchange processes in solution.

The insertion of  $N,N'$ -dicyclohexylcarbodiimide into the Mg–C bond of mesityl Grignard generates the amidinate  $\text{Mg}(\text{mesC}\{\text{NCy}\}_2)\text{Br}(\text{OEt}_2)$  (**2**). This reaction is most conveniently performed in diethyl ether, from which the product precipitates as an analytically pure white solid. No ligand distribution was evident by NMR spectroscopy, and data were consistent with a symmetrically bound amidinate.

Single-crystal X-ray crystallography confirmed **1** as the monomeric bis-THF adduct  $\text{Mg}(\text{mes})(\text{OAr})(\text{THF})_2$  (Scheme 1).† The metal is in a distorted tetrahedral geometry with a large angle between the terminal aryloxy and mesityl ligands [ $127.23(6)^\circ$ ]. The overall structure resembles  $\text{Mg}(\text{OAr})\text{Et}(\text{TMEDA})$ ,<sup>11</sup> although the aryloxy ligand in **1** approaches linearity [ $\text{Mg}-\text{O1}-\text{C10} = 165.0(1)^\circ$ ] rather than the distinctly bent geometry in the TMEDA adduct ( $146.03^\circ$ ), suggesting there is an interaction between the oxygen lone-pair and the metal.<sup>12</sup>

Structurally characterized magnesium halides supported by amidinate (one example),<sup>8b</sup> formamidinate (two examples)<sup>9b,h</sup> or guanidinate ligands (three examples)<sup>13</sup> are surprisingly rare considering the ready availability of Grignard reagents. Compound **2** dimerizes in the solid-state through  $\mu\text{-Br}$  bridges, generating five-coordinate magnesium centres. The metal geometry is best described as distorted trigonal bipyramidal ( $\tau$  value = 0.70)<sup>14</sup> with the chelating amidinate occupying the axial (N1) and equatorial (N2) positions [bite angle  $64.76(8)^\circ$ ]. Despite the difference in the relative positions of the nitrogen atoms that have previously been shown to promote the localization of  $\pi$ -electron density within the amidinate ligand,<sup>7b</sup> the carbon–nitrogen distances in the heteroallylic unit of **2** indicate symmetrical delocalization across the NCN moiety.

Compound **2** is amenable to further derivitization *via* metathesis of the bromide ligand. Reaction with  $\text{LiOAr}$  and  $\text{LiN}\{\text{SiMe}_3\}_2$  afforded  $\text{Mg}(\text{mesC}\{\text{NCy}\})(\text{OAr})(\text{THF})$  (**3**) and  $\text{Mg}(\text{mesC}\{\text{NCy}\})(\text{N}\{\text{SiMe}_3\}_2)(\text{THF})$  (**4**), respectively (Scheme 1). Both compounds are isolated as colourless crystals in good yield. Spectroscopic and analytical data are consistent with the mono-THF adduct.‡

X-Ray diffraction analysis shows similar structural features for **3** (Fig. 2) and **4**,† each consisting of a monomeric, four-coordinate magnesium with terminal aryloxy and amide ligands, respectively. The amidinate chelates symmetrically with an acute bite angle typical for this group [**3**  $65.89(9)^\circ$ ; **4**  $65.54(7)^\circ$ ]. This is compensated for by obtuse angles between the amidinate nitrogens and the  $\text{O}_{\text{aryl}}$  (average  $133.04^\circ$ ) and  $\text{N}_{\text{amide}}$  (average  $132.55^\circ$ ) atoms. The terminal aryloxy group in **3** is comparable to that in **1** with a near linear geometry at O1 [ $\text{Mg}-\text{O1}-\text{C23}$   $163.38(18)^\circ$ ]. The bis(trimethylsilyl)amido group in **4** consists of a planar nitrogen ( $\Sigma_{\text{angles}} \text{N3} = 359.7^\circ$ ), and has a Mg–N bond

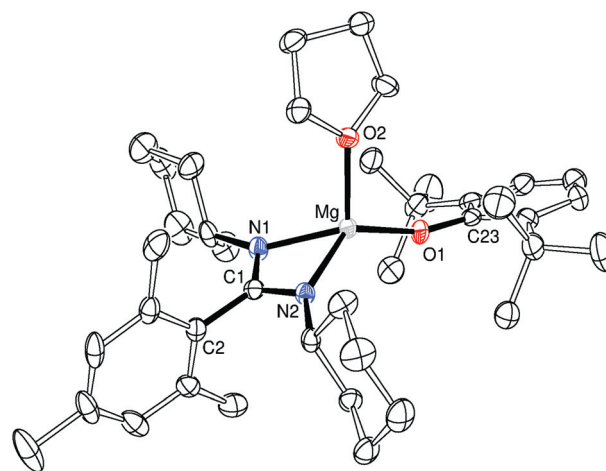


**Fig. 2** ORTEP diagrams of  $\text{Mg}(\text{mesC}\{\text{NCy}\}_2)(\text{OAr})(\text{THF})$  (**3**) (ellipsoids at 30% probability, hydrogen atoms omitted). Selected bond lengths (Å) and angles ( $^\circ$ ): Mg–N1 2.067(2), Mg–N2 2.054(2), Mg–O1 1.8431(19), Mg–O2 2.005(2), C1–N1 1.328(3), C1–N2 1.329(3); N1–Mg–N2  $65.89(9)$ , N1–Mg–O1  $134.82(10)$ , N2–Mg–O1  $131.25(9)$ , O1–Mg–O2  $103.07(9)$ , Mg–O1–C23  $163.38(18)$ .

identical (within  $3\sigma$ ) from that reported in the hpp- and tbo-derivatives **A** and **B**.<sup>6</sup>

Preliminary NMR scale analysis using benzaldehyde confirms that **3** and **4** promote the Tishchenko reaction.† At 1 mol% catalyst loading, the yield of ester produced by amide **4** after 10 min was 37% (TOF  $\sim 220 \text{ h}^{-1}$ ),<sup>15</sup> compared with 20% yield (TOF  $120 \text{ h}^{-1}$ ) produced by **A** and **B**.<sup>6</sup> After an additional 20 min the yield was 65%, rising to 74% after 60 min.§ Compound **4** also promoted ester formation under solvent-free conditions, giving a yield of 98% benzylbenzoate after 24 h.

NMR scale reactions using 1 mol% of **4** and 2,2-dimethylpropanal (pivaldehyde) demonstrate increased performance compared to **A**. For example, the yields of 2,2-dimethylpropyl-2,2-dimethylpropanoate after 10 min are 10% and 25% (TOF  $60 \text{ h}^{-1}$  and  $150 \text{ h}^{-1}$ ) for **A** and **4**, respectively, with a greater than 95% yield produced by **4** after 3 h (*cf.* 62% for **A**).

The catalytic profile for the dimerization of cyclohexanecarbaldehyde using **A** and **4** is very similar. The initial production of cyclohexylcyclohexanoate is rapid with both compounds, with 51% and 48% yield (TOF  $\sim 300 \text{ h}^{-1}$ ) for **A** and **4**, respectively. However, the data suggests the formation of side-products as the yield of ester produced by **4** is only  $\sim 60\%$  when all of the aldehyde has been consumed. The attempted dimerization of ethanal (acetaldehyde) and 2-methylpropanal (isobutyraldehyde) gave only complex mixtures.

In contrast to the dimerization of benzaldehyde promoted by **4**, the aryloxy **3** produces benzylbenzoate at a much lower rate. After 10 min there is no detectable amount of ester, and the yield is only 15% after 60 min. Assuming that complex **3** is the *pre*-catalyst for this reaction and that the active species is the alkoxide  $[\text{Mg}(\text{mesC}\{\text{NCy}\}_2)(\text{OCH}_2\text{Ph})(\text{L})_n]$  (**I**,  $\text{L} = \text{neutral donor}$ ),<sup>2,6</sup> these results suggest that the initial reaction of **3** with benzaldehyde is slow and only a small amount is converted to **I** under these conditions. We sought to exploit this slow initiation of **3** with aldehyde to isolate compounds that may be representative of the intermediates produced during the catalytic cycle.

The reaction of **3** with two equivalents of 2,4,6-trimethylbenzaldehyde (mesitylaldehyde) immediately forms a bright orange solution, from which crystals of **5** were isolated. The  $^1\text{H}$  and  $^{13}\text{C}$   $\{^1\text{H}\}$  NMR spectra of **5** show resonances at  $\delta_{\text{H}}$  10.50 ppm and  $\delta_{\text{C}}$  197.2 ppm, respectively, indicative of an aldehyde functionality. The remaining resonances for the amidinate ligand and mesityl group indicate a symmetrical environment at magnesium.

The X-ray crystal structure of **5** (Fig. 3) shows a five-coordinate magnesium centre bonded to a chelating amidinate ligand, a terminal aryloxy and two mesitylbenzaldehyde molecules. The geometry is closest to square-based pyramidal ( $\tau$  value = 0.25) with O2 defining the apex, although the planarity of the amidinate metallacycle and the small bite angle result in a significant twist between the planes defined by Mg,N1,N2 and Mg,O2,O3 [39.7°]. The Mg–O<sub>aryl</sub> distance is longer than in the THF adduct **3**, with a concomitant increase in the angle at O1. Although these data are consistent with a weakening of the metal–aryloxy bond, which is required for the generation of the active catalyst **I**, this is more likely to represent the increased coordination number in **5**.

The orientation of the aldehyde ligands suggests that coordination is through an  $\text{sp}^2$ -type lone pair on the oxygen atoms, with C–O<sub>aldehyde</sub>–Mg angles  $\sim 124^\circ$ . The Mg–O<sub>aldehyde</sub> bond lengths in **5** are similar to that in the *para*-isopropylbenzaldehyde adduct  $[\text{Mg}(\mu\text{-OAr})\text{Br}(\text{OEt})_2(4\text{-}^i\text{PrC}_6\text{H}_4\text{COH})_2]_2$ ,<sup>16</sup> and there is no appreciable lengthening of the C=O bond lengths compared with other examples of metal mesC(O)H adducts.<sup>17</sup>

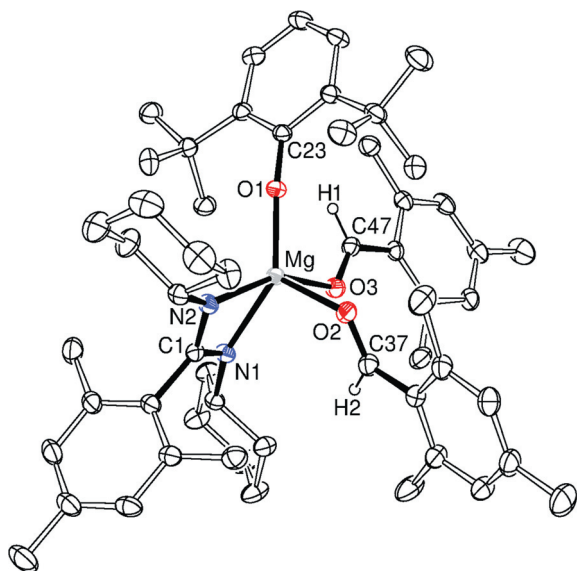


**Fig. 3** ORTEP diagram of  $\text{Mg}(\text{mesC}\{\text{NCy}\}_2)(\text{OAr})(\text{mesCHO})_2$  (**5**) (ellipsoids at 30% probability, hydrogen atoms except aldehyde protons and solvate molecules omitted). Selected bond lengths (Å) and angles ( $^\circ$ ): Mg–O1 1.8842(13), Mg–N1 2.0967(15), Mg–N2 2.1184(15), Mg–O2 2.0780(14), Mg–O3 2.1566(13), O1–C23 1.322(2), O2–C37 1.228(2), O3–C47 1.231(2), C1–N1 1.336(2), C1–N2 1.324(2); N1–Mg–N2 64.14(6), N1–Mg–O1 141.21(6), N1–Mg–O2 104.30(6), N1–Mg–O3 93.38(6), N2–Mg–O1 110.13(6), N2–Mg–O2 93.07(6), N2–Mg–O3 156.06(6), O1–Mg–O2 114.43(6), O1–Mg–O3 92.44(5), O2–Mg–O3 84.31(5), Mg–O1–C23 164.09(12), Mg–O2–C37 124.71(12), Mg–O3–C47 124.23(12).

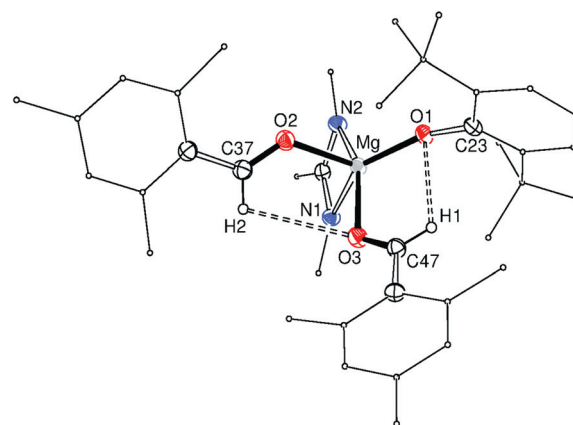


**Fig. 4** Core structure of **5** showing intramolecular hydrogen bonds.

The core structure of **5** is stabilized by intramolecular hydrogen-bonding between H1...O1 (2.54 Å) and H2...O3 (2.91 Å) (Fig. 4).

The accessibility of bis-aldehyde adducts at a five-coordinate metal have not been considered when describing the mechanism of the Tishchenko reaction promoted by magnesium, likely due to the small size of the metal. However, this result in combination with the different catalytic profile observed for **3** compared with **4**, may indicate an alternative catalytic pathway is operating in this instance. Further tests are being carried out to determine the mechanism, where preliminary results indicate that heating an NMR sample of **5** produces the ester in the absence of additional aldehyde, suggesting the bis(aldehyde) may be considered an intermediate in the catalysis promoted by magnesium amidinate compounds.

## Notes and references

‡ Despite repeated attempts, accurate elemental analysis could not be obtained for compounds **1** and **3**. We believe that in the case of **3** this is due to inefficient removal of the LiBr side product (see ESI for the  $^1\text{H}$  and  $^{13}\text{C}$  NMR spectra).

§ The reduction in the rate of ester production is likely to be due to more competitive binding of the THF at high conversions, where the concentration of aldehyde is low.

- W. Tishchenko, *Chem. Zentralbl.*, 1906, **77**, 1309–1311.
- T. Seki, T. Nakajo and M. Onaka, *Chem. Lett.*, 2006, **35**, 824–829.
- M. R. Crimmin, A. G. M. Barrett, M. S. Hill and P. A. Procopiou, *Org. Lett.*, 2007, **9**, 331–333.
- (a) L. Cronin, F. Manoni, C. J. O'Connor and S. J. Connon, *Angew. Chem., Int. Ed.*, 2010, **49**, 3045–3048; (b) C. J. O'Connor, F. Manoni, S. P. Curran and S. J. Connon, *New J. Chem.*, 2011, **35**, 551–553; (c) S. P. Curran and S. J. Connon, *Org. Lett.*, 2012, **14**, 1074–1077.
- M. P. Coles, *Chem. Commun.*, 2009, 3659–3676.
- B. M. Day, N. E. Mansfield, M. P. Coles and P. B. Hitchcock, *Chem. Commun.*, 2011, **47**, 4995–4997.
- (a) R. Lechler, H.-D. Hausen and J. Weidlein, *J. Organomet. Chem.*, 1989, **359**, 1–12; (b) M. P. Coles, D. C. Swenson, R. F. Jordan and V. G. Young Jr., *Organometallics*, 1997, **16**, 5183–5194.
- (a) B. Srinivas, C.-C. Chang, C.-H. Chen, M. Y. Chiang, I.-T. Chen, Y. Wang and G.-H. Lee, *J. Chem. Soc., Dalton Trans.*, 1997, 957–963; (b) J. A. R. Schmidt and J. Arnold, *J. Chem. Soc., Dalton Trans.*, 2002, 2890–2899.
- (a) M. Westerhausen and H.-D. Hausen, *Z. Anorg. Allg. Chem.*, 1992, **615**, 27–34; (b) F. A. Cotton, S. C. Haefner, J. H. Matonic, X. Wang and C. A. Murillo, *Polyhedron*, 1997, **16**, 541–550; (c) D. Walther, P. Gebhardt, R. Fischer, U. Kreher and H. Görls, *Inorg. Chim. Acta*,

- 1998, **281**, 181–189; (d) A. R. Sadique, M. J. Heeg and C. H. Winter, *Inorg. Chem.*, 2001, **40**, 6349–6355; (e) M. L. Cole, D. J. Evans, P. C. Junk and L. M. Louis, *New J. Chem.*, 2002, **26**, 1015–1024; (f) A. Xia, H. M. El-Kaderi, M. J. Heeg and C. H. Winter, *J. Organomet. Chem.*, 2003, **682**, 224–232; (g) R. T. Boéré, M. L. Cole and P. C. Junk, *New J. Chem.*, 2005, **29**, 128–134; (h) P. C. Andrews, M. Brym, C. Jones, P. C. Junk and M. Kloth, *Inorg. Chim. Acta*, 2006, **359**, 355–363; (i) N. Nimitsiriwat, V. C. Gibson, E. L. Marshall, P. Takolpuckdee, A. K. Tomov, A. J. P. White, D. J. Williams, M. R. J. Elsegood and S. H. Dale, *Inorg. Chem.*, 2007, **46**, 9988–9997.
- 10 K. W. Henderson, G. W. Honeyman, A. R. Kennedy, R. E. Mulvey, J. A. Parkinson and D. C. Sherrington, *Dalton Trans.*, 2003, 1365–1372.
- 11 A. D. Pajerski, E. P. Squiller, M. Parvez, R. R. Whittle and H. G. Richey Jr., *Organometallics*, 2005, **24**, 809–814.
- 12 J. Calabrese, M. A. Cushing Jr. and S. D. Ittel, *Inorg. Chem.*, 1988, **27**, 867–870.
- 13 (a) J. Cheng, *Acta Crystallogr., Sect. E: Struct. Rep. Online*, 2011, **67**, m987; (b) O. Ciobanu, A. Fuchs, M. Reinmuth, A. Lebkücher, E. Kaifer, H. Wadepl and H.-J. Himmel, *Z. Anorg. Allg. Chem.*, 2010, **636**, 543–550; (c) S. P. Green, C. Jones and A. Stasch, *Science*, 2007, **318**, 1754–1757.
- 14 A. W. Addison, T. N. Rao, J. Reedijk, J. van Rijn and G. C. Verschoor, *J. Chem. Soc., Dalton Trans.*, 1984, 1349–1356.
- 15 J. Takehara, S. Hashiguchi, A. Fujii, S. Inoue, T. Ikariya and R. Noyori, *Chem. Commun.*, 1996, 233–234.
- 16 G. Bocelli, A. Cantoni, G. Sartori, R. Maggi and F. Bigi, *Chem.–Eur. J.*, 1997, **3**, 1269–1272.
- 17 B. Müller and H. Vahrenkamp, *Eur. J. Inorg. Chem.*, 1999, 117–127.